Redox Pathways in DNA Oxidation: Kinetic Studies of Guanine and Sugar Oxidation by Para-Substituted Derivatives of Oxoruthenium(IV)

Brian T. Farrer and H. Holden Thorp*

Department of Chemistry, University of North Carolina, Chapel Hill, North Carolina 27599-3290

Received July 14, 1999

The oxidation of nucleotides and DNA by a series of complexes based on $Ru(tpy)(bpy)O^{2+}$ (**1**) was investigated (tpy = 2,2′:6′,2″-terpyridine; bpy = 2,2′-bipyridine). These complexes were substituted with electron-donating or -withdrawing substituents in the para positions of the polypyridyl ligands so that the oxidation potentials of the complexes were affected but the reaction trajectory of the oxo ligand with DNA was the same throughout the series. The prepared complexes were (with $E_{1/2}$(III/II) and $E_{1/2}$(IV/III) values in volts versus Ag/AgCl) Ru(4′-EtO-tpy)(bpy)O^{2+} (**2**; 0.47, 0.60), Ru(4′-Cl-tpy)(bpy)O^{2+} (**3**; 0.55, 0.63), Ru(tpy)(4,4′-Me_2-bpy)O^{2+} (**4**; 0.48, 0.62), and Ru(tpy)(4,4′-Cl_2-bpy)O^{2+} (**5**; 0.58, 0.63). The complexes oxidized deoxycytosine 5′-monophosphate at the sugar moiety (k = 0.24−0.47 M^{-1} s^{-1}) and guanosine 5′-monophosphate at the base moiety (k = 6.1−15 M^{-1} s^{-1}). The rate constants increase across these ranges in the order **3** > **1** > **4** > **2**, which is the same order as the redox potentials of the complexes. The effect of the base on these reactions was also studied, and xanthine was found to react with **1** much faster than guanine while hypoxanthine was less reactive than the sugar moiety. The complexes all oxidized oligonucleotides to generate base-labile lesions at guanine and a combination of spontaneous and base-labile scission at the sugar functionalities. The selectivity of cleavage in duplex and single-stranded DNA was not a strong function of the substituents on the metal complex.

Introduction

Oxidizing metal complexes that damage DNA have been studied intensively.[1−3] The details of investigation in this field are in a mature state where detection of products and analysis of single sites of reaction by high-resolution electrophoresis are common.[4−6] This level of mechanistic detail has provided insight into the general mechanisms by which nucleic acids are damaged by radiation, natural mutagens, and chemotherapeutic agents.[4,7−9] Among the many systems characterized in this manner are oxomanganese porphyrins,[1] oxochromium complexes,[10] high-valent nickel species,[4] and oxidizing excited states based on polypyridyl complexes of rhodium(III).[5] We have studied the DNA oxidation chemistry of complexes based on Ru(tpy)(bpy)-O^{2+} (bpy = 2,2′-bipyridine; tpy = 2,2′:6′,2″-terpyridine),[3,11] which have the advantages that the redox kinetics can be followed independently by optical spectroscopy and that authentic samples of the oxidizing form can be prepared and quantitated.

In previous studies, we have shown that complexes based on $Ru(tpy)(bpy)O^{2+}$ oxidize DNA via two competing pathways.[12] The first involves oxidation of the 1′ C−H bond to generate a combination of spontaneous and base-labile scission according to[12]

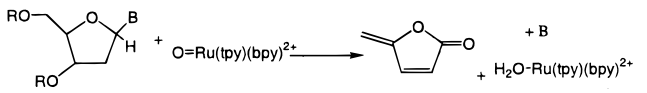

(1)

We have detected the 5-methylenefuranone product and shown by isotopic labeling that a majority of the ketone oxygen is derived from the oxo ligand of the ruthenium complex.[13] The parallel guanine oxidation pathway is less well characterized, but produces alkali-labile scission with significantly greater efficiency than the sugar oxidation pathway.[12] Because the sugar oxidation pathway is attenuated by polar substituents on the 2′ position, only guanine oxidation is observed in RNA where there is a 2′-OH group.[13] In addition, we have shown that the guanine oxidation reaction is more sensitive to the secondary structure, and there is a high selectivity for guanines in single-stranded regions, such as loops and bulges, in nucleic acids of complex structures.[13] For example, the simple $Ru(tpy)(bpy)O^{2+}$ complex selectively oxidized a single guanine in the loop of the iron-responsive element upon reaction with the entire (500 nucleotide) ferritin messenger RNA.[14,15]

In this study, greater mechanistic detail on the oxidation of nucleic acids by $Ru(tpy)(bpy)O^{2+}$ was obtained by substituting

(1) Meunier, B. *Chem. Rev.* **1992**, *92*, 1411.
(2) Burrows, C. J.; Rokita, S. E. *Acc. Chem. Res.* **1994**, *27*, 295−301.
(3) Thorp, H. H. *Adv. Inorg. Chem.* **1995**, *43*, 127−177.
(4) Duarte, V.; Muller, J. G.; Burrows, C. J. *Nucleic Acids Res.* **1999**, *27*, 496−502.
(5) Sitlani, A.; Long, E. C.; Pyle, A. M.; Barton, J. K. *J. Am. Chem. Soc.* **1992**, *114*, 2303.
(6) Pitié, M.; Bernadou, J.; Meunier, B. *J. Am. Chem. Soc.* **1995**, *117*, 2935−2936.
(7) Greenberg, M. *Chem. Res. Toxicol.* **1998**, *11*, 1235−1248.
(8) Beckman, K. B.; Ames, B. N. *J. Biol. Chem.* **1997**, *272*, 19633−19636.
(9) Hecht, S. M. *Bioconjugate Chem.* **1994**, *5*, 513−526.
(10) Bose, R. N.; Moghaddas, S.; Mazzer, P. A.; Dudones, L. P.; Joudah, L.; Stroup, D. *Nucleic Acids Res.* **1999**, *27*, 2219−2226.
(11) Grover, N.; Thorp, H. H. *J. Am. Chem. Soc.* **1991**, *113*, 7030.
(12) Cheng, C.-C.; Goll, J. G.; Neyhart, G. A.; Welch, T. W.; Singh, P.; Thorp, H. H. *J. Am. Chem. Soc.* **1995**, *117*, 2970−2980.
(13) Carter, P. J.; Cheng, C.-C.; Thorp, H. H. *J. Am. Chem. Soc.* **1998**, *120*, 632−642.
(14) Ciftan, S. A.; Theil, E. C.; Thorp, H. H. *Chem. Biol.* **1998**, *5*, 679−687.
(15) Thorp, H. H.; McKenzie, R. A.; Lin, P.-N.; Walden, W. E.; Theil, E. C. *Inorg. Chem.* **1996**, *35*, 2773−2779.

10.1021/ic990833u CCC: $19.00
Published on Web 12/15/1999

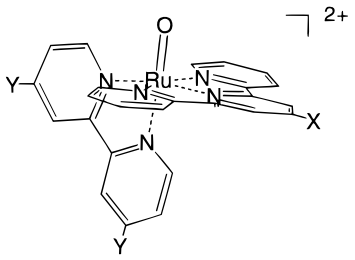

Compound	X	Y
1	H	H
2	CH_3CH_2O	H
3	Cl	H
4	H	CH_3
5	H	Cl

Figure 1. Structures of complexes studied: **1** = Ru(tpy)(bpy)O^{2+}, **2** = Ru(EtO-tpy)(bpy)O^{2+}, **3** = Ru(Cl-tpy)(bpy)O^{2+}, **4** = Ru(tpy)(Me_2-bpy)O^{2+}, **5** = Ru(tpy)(Cl_2-bpy)O^{2+}.

at the 4′ position of the polypyridyl rings (Figure 1), changing the electronic properties of the oxidant but minimally perturbing the coordination environment of the reactive oxo ligand. The results further support our understanding of the 1′-hydride abstraction for sugar oxidation and electrophilic attack on the guanine base. Although the guanine oxidation by Ru(tpy)(bpy)-O^{2+} is clearly an inner-sphere reaction, the trend in relative rates follows that of the one-electron ionization potentials.

Experimental Section

Materials. 2,2′:6′,2″-Terpyridine (tpy), 2,2′-bipyridine (bpy), 4,4′-Me_2-bpy, $RuCl_3 \cdot xH_2O$, and D_2O (99.9 atom %) were purchased from Aldrich Chemical Co. 4′-Cl-tpy and 4′-EtO-tpy were prepared as demonstrated by Constable et al.[16] 4,4′-Cl_2-bpy was prepared by the method published by Cook et al.[17] Na_2HPO_4 and NaH_2PO_4 were purchased from Mallinckrodt and used without further purification. Water was house distilled and further purified by passage through a Millipore Milli-Q water purification system. Glassy carbon working electrodes were purchased from Bioanalytical Systems (BAS). Vitreous carbon working electrodes were purchased from The Electrosynthesis Co. Ag/AgCl reference electrodes were purchased from Cypress Systems. The [Ru(4′-X-tpy)(4,4′-Y_2-bpy)O]$(ClO_4)_2$ complexes were prepared analogously to the synthesis of [Ru(tpy)(bpy)O]$(ClO_4)_2$[18] except Cl_2 instead of Br_2 was used as the oxidant in the final step.[19] The resulting oxo complex was dried in vacuo for 1 h to allow handling. *Warning! Perchlorate salts of metal complexes containing organic ligands are potentially explosive when subjected to rigorous drying.* Anal. Found (Calcd): [Ru(4′-EtO-tpy)(bpy)O]$(ClO_4)_2$ (**2**)] C, 42.27 (43.2); H, 3.27 (3.09); N, 8.93 (9.34). [[Ru(4′-Cl-tpy)(bpy)O]$(ClO_4)_2$ (**3**)] C, 40.13 (40.6); H, 2.52 (2.50); N, 9.39 (9.50). [Ru(tpy)(4,4′-$(CH_3)_2$-bpy)O]$(ClO_4)_2$ (**4**)] C, 43.47 (44.21); H, 3.35 (3.16); N, 9.40 (9.54). [[Ru(tpy)(4,4′-Cl_2-bpy)O]$(ClO_4)_2 \cdot H_2O$ (**5**)] C, 37.4 (37.8); H, 2.27 (2.41); N, 8.71 (8.83). (*Note:* [Ru(tpy)(4,4′-$(CH_3)_2$-bpy)O]$(ClO_4)_2$ and [Ru(4′-EtO-tpy)(bpy)O]$(ClO_4)_2$ were sent in a desiccator to Atlantic Microlab, Inc.)

Electrochemistry. Cyclic voltammetry was carried out on a PAR Model 273A potentiostat scanning from 100 to 900 mV at 20 mV/s using a glassy carbon working electrode and Ag/AgCl reference and Pt wire counter. Solutions of the $RuOH_2^{2+}$ form were made by dissolving a small amount of $RuOH_2^{2+}$ in 50 mM sodium phosphate buffer, pH 7.8. The concentration of ruthenium was determined using the extinction coefficient at the maximum of the MLCT band at around 480 nm. Values of $E_{1/2}$ were determined from averages of the peak potentials or by fitting to two redox couples with the COOL algorithm; experimentally identical values were determined by either method.

Spectroscopy. Spectroelectrochemistry was carried out on the $RuOH_2^{2+}$ complexes to determine the spectra of the three oxidation states. A three-compartment cell with a quartz UV−vis cell attached to the middle cell was used. Slow cyclic voltammagrams were performed on a PAR Model 273A potentiostat scanning from 0.200 to 0.900 V (vs Ag/AgCl) at 0.1 mV/s using a vitreous carbon working electrode (middle compartment) and a platinum counter electrode (left compartment) in 50 mM sodium phosphate buffer (pH 7.1), resulting in a net bulk electrolysis. Visible spectra (340−510 nm) were taken on a Hewlett-Packard 8452A diode array spectrophotometer at 2 min intervals during the voltage sweep. The resulting spectra were imported into SPECFIT (Spectrum Software Associates, Chapel Hill, NC) and split into the forward and reverse waves. The data were then analyzed via an Evolving Factor Analysis algorithm incorporated in the program SPECFIT to obtain spectra of the Ru^{II}, Ru^{III}, and Ru^{IV} for each of the substituents.

Kinetics. The reaction of the ruthenium oxo species with guanine 5′-monophosphate was monitored using an OLIS-RSM stopped-flow spectrophotometer scanning at 32 scans/s for 10 s. The reactions were carried out in 50 mM phosphate buffer (pH 7). The reactions were observed to be first order with respect to [5′-GMP], and rate constants were obtained from plotting the initial rate vs [5′-GMP] and taking the slope to be k[RuO^{2+}]. Initial rates were obtained by using the kinetic trace at the Ru(II)/Ru(III) isosbestic point around 410 nm, allowing the loss of RuO^{2+} to be observed directly. d[RuO^{2+}]/dt was obtained from dA/dt using the relation d[RuO^{2+}]/dt = $-\{1/[(\epsilon_{II} - \epsilon_{IV})b]\}$ dA/dt. Here ϵ_{II} and ϵ_{IV} are the extinction coefficients of Ru(II)OH_2^{2+} and Ru(IV)O^{2+}, respectively, and b is the path length of the cell (1.8 cm). The kinetics of 2′-deoxycytidine 5′-monophosphate oxidation were also followed using an Olis-RSM spectrophotometer. Data were collected over 30 min taking 1 scan/s in 50 mM phosphate buffer (pH 7). The data were fit using the global analysis program SPECFIT using the model kinetic scheme

$$A \xrightarrow{k_{obs}} B \tag{2}$$

$$A \underset{k_d}{\overset{k_c}{\rightleftharpoons}} B \tag{3}$$

This model was used because it is kinetically identical to the proposed oxidation mechanism[20]

$$RuO^{2+} + dCMP^{2-} \overset{K_b}{\rightleftharpoons} RuO^{2+} \cdot dCMP^{2-} \tag{4}$$

$$RuO^{2+} \cdot dCMP^{2-} \xrightarrow{k} RuOH_2^{2+} + dCMP_{ox}^{2-} \tag{5}$$

$$RuO^{2+} + RuOH_2^{2+} \underset{k_d}{\overset{k_c}{\rightleftharpoons}} 2RuOH^{2+} \tag{6}$$

under pseudo-first-order conditions in [RuO^{2+}] and rapid equilibration of the preassociation complex in eq 4. If [$dCMP^{2-}$] is low enough that saturation of RuO^{2+} does not occur, eqs 4 and 5 can be estimated as a single second-order step (where k_{obs} for low [$dCMP^{2-}$] is equivalent to $K_b k$[CMP^{2-}]). Values for the comproportionation and disproportionation rate constants, k_c and k_d, were taken from data previously reported. k_{obs} was then plotted against [$dCMP^{2-}$], and the slope of this plot was taken to be the second-order rate constant $K_b k$.

(16) Constable, E. C.; Thompson, A. M. *New J. Chem.* **1992**, *16*, 855−867.
(17) Cook, M. J.; Lewis, A. P.; McAuliffe, G. S. G.; Skarda, V.; Thomson, A. J.; Glasper, J. L.; Robbins, D. J. *J. Chem. Soc., Perkins Trans. 2* **1984**, 1293−1301.
(18) Takeuchi, K. J.; Thompson, M. S.; Pipes, D. W.; Meyer, T. J. *Inorg. Chem.* **1984**, *23*, 1845.
(19) Welch, T. W.; Neyhart, G. A.; Goll, J. G.; Ciftan, S. A.; Thorp, H. H. *J. Am. Chem. Soc.* **1993**, *115*, 9311−9312.
(20) Neyhart, G. A.; Cheng, C.-C.; Thorp, H. H. *J. Am. Chem. Soc.* **1995**, *117*, 1463−1471.

Table 1. Properties of Oxoruthenium(IV) Complexes and Rate Constants for Reaction with Nucleotides in Aqueous Solution at Room Temperature

compound	E(III/II) (V)[a]	E(IV/III) (V)[a]	λ_{max}(Ru(II)) (nm)	k_G (M^{-1} s^{-1})[b]	k_{sug} (M^{-1} s^{-1})[c]	k_G/k_{sug}
Ru(EtO-tpy)(bpy)O^{2+} (**2**)	0.47	0.60	480	6.1 ± 0.4	0.24 ± 0.02	26
Ru(tpy)(Me_2-bpy)O^{2+} (**4**)	0.48	0.62	478	6.6 ± 0.6	0.29 ± 0.02	22
Ru(tpy)(bpy)O^{2+} (**1**)	0.49	0.62	476	8.1 ± 0.6	0.31 ± 0.01	26
Ru(Cl-tpy)(bpy)O^{2+} (**3**)	0.55	0.63	478	15 ± 1	0.47 ± 0.03	22
Ru(tpy)(Cl_2-bpy)O^{2+} (**5**)	0.58	0.63	492	*d*	*d*	*d*

[a] Determined by cyclic voltammetry and fitting with two oxidation processes; see the text. [b] Determined by initial rate analysis from mixing the Ru(IV)O^{2+} complex with guanosine 5′-monophosphate. [c] Determined from fitting spectral changes in the reaction of the oxo complex with deoxycytosine 5′-monophosphate to the mechanism shown in eqs 11 and 12. [d] The spontaneous decomposition of Ru(tpy)(Cl_2-bpy)O^{2+} was faster than the reaction with nucleotides and precluded determination of the reaction rate constants.

DNA Oxidation. DNA was 5′-end-labeled as described elsewhere.[12] Single- and double-stranded DNA stock solutions were prepared by mixing 50 μL of 5′-^{32}P-end-labeled **DNA1** sequence (5′-ATGCC-$CTTGCG_{11}$TAT-3′), 10 μL of 100 μM unlabeled **DNA1**, and 20 μL of 50 mM sodium phosphate buffer (pH 7) with either 20 μL of water (in the case of single-stranded DNA) or 11 μL of 100 μM **DNA2** (5′-ATACGCAAGGGCAT-3′) and 9 μL of water (in the case of double-stranded DNA) for a final DNA concentration of 33 μM in nucleotide phosphate. For double-stranded DNA, the solution was heated to 90 °C and allowed to cool slowly to the temperature of the experiment. The extent of hybridization was checked by adding 10 μL of a 30 μM competitive complementary strand in 10 mM sodium phosphate buffer (pH 7) and comparing the volume of the respective bands on a 20% polyacrylamide nondenaturing gel. A stock solution of [Ru(4′-X-tpy)-(4,4′-Y_2-bpy)O](ClO_4)$_2$ was made by dissolving a small amount of the complex in 50 mM sodium phosphate buffer (pH 6.8). This solution was held at a potential of +0.85 V (vs Ag/AgCl, Pt wire counter, vitreous carbon working) to ensure the absence of lower oxidation state Ru. This solution was then diluted by a factor of 5 with water (final buffer concentration 10 mM). This solution (0−10 μL) was added to a solution of 10 μL of oligonucleotide (14 μM) in water and 10 μL sodium phosphate buffer (pH 6.8), a total solution volume of 20 μL. The reaction was allowed to proceed for 10 min at room temperature when 800 μL of cold (−4 °C) ethanol was added to quench the reaction. Sodium acetate (1.5 M, 20 μL) was added, and the solution was placed on dry ice for 30 min to precipitate the DNA. After centrifugation, the solutions were lyophilized to produce a white pellet that was piperidine treated using literature methods.[12] Resulting pellets were dissolved in 10 μL of gel loading buffer (80% formamide in water with 0.0025% bromophenol blue and 0.0025% xylene cyanol FF) and run on a 20% polyacrylamide denaturing gel using an established protocol.[21] The resulting polyacrylamide gels were imaged using Molecular Dynamics phosphorimaging screens. The screens were scanned using a Molecular Dynamics Storm 840 phosphorimager. Analysis of the resulting images was performed using ImageQuant by drawing equivalent rectangles around each of the cleavage bands and integrating the band intensity within the rectangle. The volumes were then plotted against [RuO^{2+}], and slopes of the lines were taken as an indicator of the relative rates of reaction of the nucleotides with RuO^{2+}.

Results

Syntheses and Properties of Ru(4′-X-tpy)(4,4′-Y_2-bpy)O]-(ClO_4)$_2$. The 4′-chloroterpyridine is commercially available, and the 4′-ethoxyterpyridine and 4,4′-dichlorobypyridine can be prepared using known reactions.[16,17] The syntheses of [Ru(4′-X-tpy)(4,4′-Y_2-bpy)O](ClO_4)$_2$ were then carried out similarly to the published procedure for [Ru(tpy)(bpy)O](ClO_4)$_2$ by reaction of the bpy derivative with the Ru(tpy)Cl_3 derivative under reducing conditions followed by conversion to the aqua complex with $AgClO_4$.[18] The resulting Ru(4′-X-tpy)(4,4′-Y_2-bpy)OH_2^{2+} complexes were then oxidized to the oxo complexes using chlorine gas as an oxidant.[19]

The electrochemistry of the $RuOH_2^{2+}$ compounds consists of two one-electron oxidations both coupled to proton loss to ultimately give the ruthenium oxo compounds:[18]

$$Ru(II)OH_2^{2+} \rightleftharpoons Ru(III)OH^{2+} + e^- + H^+ \quad (7)$$

$$Ru(III)OH^{2+} \rightleftharpoons Ru(IV)O^{2+} + e^- + H^+ \quad (8)$$

Both of these reactions are reversible, so when bulk electrolysis is performed on solutions of the Ru(II)OH_2^{2+} complexes, the optical spectra of all three oxidation states can be obtained. The redox potentials for eqs 7 and 8 of all the substituted complexes were measured by spectroelectrochemistry, and the results for pH 7 are given in Table 1. The reduction potentials obtained by this method were similar to those obtained by conventional cyclic voltammetry and show that the potential of the III/II couple is more sensitive to the substituents than that of the IV/III couple. This observation is presumably due to the greater electron-donating ability of the oxo ligand compared to that of the hydroxo ligand, which overwhelms the electronic effect of the more distant substituent.

The complete optical spectra of all three oxidation states for each complex are given in the Supporting Information, and the λ_{max} values for the Ru(II) species are given in Table 1. Of the four substituted complexes studied, the only significant deviation from λ_{max} for the Ru(II) form compared to the parent unsubstituted complex is for Ru(tpy)(4,4′-Cl_2-bpy) OH_2^{2+}, which exhibits an MLCT band at 492 nm. This red shift supports an assignment of the bipyridine as the acceptor of the MLCT. The chlorine substituents on the bipyridine ligand lower the energy of the π^* orbitals, decreasing the energy gap between the filled $d_{xy,xz,yz}$ orbitals and the π^* orbital accepting the charge transfer.

Kinetics of Nucleotide Oxidation. Oxoruthenium(IV) polypyridyl complexes oxidize nucleic acids at both the base and sugar moieties.[3] Base oxidation occurs primarily at guanine to produce base-labile lesions, and sugar oxidation occurs via oxidation of the 1′-hydrogen in a base-independent manner.[12,20] The kinetics of this latter reaction were investigated with the substituted complexes using 2′-deoxycytosine 5′-monophosphate ($dCMP^{2-}$) as a model nucleotide, since the reaction of Ru(IV)-O^{2+} with the cytidine base is negligible.[20] Under conditions where [$dCMP^{2-}$] is small enough that the formation of the $dCMP^{2-}$·RuO^{2+} ion pair can be neglected (eq 4), the appropriate kinetic scheme is

$$RuO^{2+} + dCMP^{2-} \rightarrow RuOH_2^{2+} + dCMP_{ox}^{2-} \quad (9)$$

$$RuO^{2+} + RuOH_2^{2+} \rightleftharpoons 2RuOH^{2+} \quad (10)$$

Fortunately, the equilibrium constant for ion-pair formation between Ru(IV)O^{2+} and $dCMP^{2-}$ is low enough that pseudo-first-order conditions can be realized (where $dCMP^{2-}$ is in

(21) Maniatis, T.; Fritsch, E. F.; Sambrook, J. *Molecular Cloning: A Laboratory Manual*, 2nd ed.; Cold Spring Harbor Press: Plainview, NY, 1989.

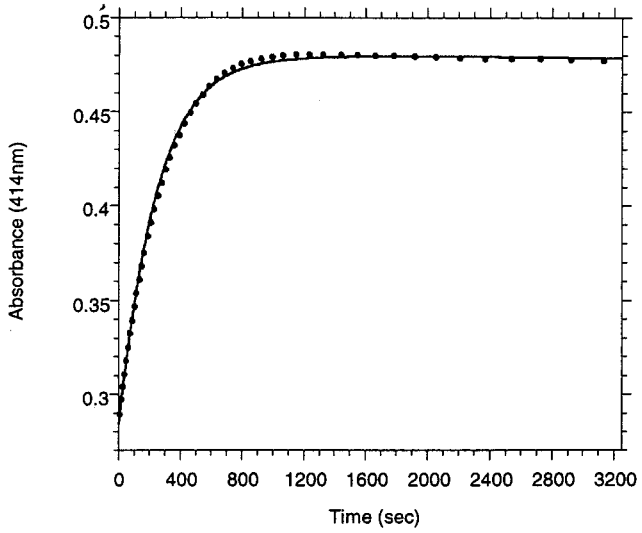

Figure 2. Kinetic trace of the absorbance at 414 nm for the oxidation of dCMP (3.0 mM) by Ru(Cl-tpy)(bpy)O^{2+} (**3**) (120 μM). The solid line is the fit determined using the mechanism shown in eqs 11 and 12.

excess), while still avoiding significant ion-pair formation. In this case, the kinetics can be described by

$$RuO^{2+} \xrightarrow{k_{obs}[dCMP]} RuOH_2^{2+} \qquad (11)$$

$$RuO^{2+} + RuOH_2^{2+} \underset{k_d}{\overset{k_c}{\rightleftharpoons}} 2RuOH^{2+} \qquad (12)$$

Since k_c and k_d have been independently obtained,[22] it is straightforward to obtain $k_{obs}[dCMP^{2-}]$ using global analysis and observing the change in the visible absorbance spectrum over time. A sample fit is shown in Figure 2 for **3**. By varying $[dCMP^{2-}]$, a series of first-order rate constants can be obtained and plotted linearly against $[dCMP^{2-}]$ to yield a slope of k_{obs}. Data collected on four of the five compounds (Figure 3A) show small differences in rate constants in the order **3** > **1** > **4** > **2**. The rate constants for these complexes are shown in Table 1. The strongly oxidizing Ru(tpy)(4,4′-Cl_2-bpy)O^{2+} (**5**) complex decomposed faster than the sugar oxidation and is not included in the series. Although the difference between the rate constants is small, the trend shown in Table 1 further supports a mechanism where oxo addition to the sugar produces significant cationic character at the 1′ position.

The molecular mechanism for guanine oxidation is complex, since guanine can donate at least four electrons, and many of the oxidation products are more reactive than guanine itself.[4,8,23] The kinetics for the oxidation of guanine by oxoruthenium(IV) have been fit previously to a complicated model involving overoxidation of guanine and direct reactions of both Ru(IV)-O^{2+} and Ru(III)OH^{2+}.[20] We show here that analysis of the kinetic data can be simplified by considering only the initial rate of the reaction and that the results for the rate-determining step are identical to those obtained using the complex model. Initial rate analysis performed for data on the first 1 s of oxidation of 5′-GMP by Ru(tpy)(bpy)O^{2+} gave a rate for the initial step of 8 ± 2 M^{-1} s^{-1} (Figure 3B). This initial rate constant compares favorably with that of 9 ± 2 M^{-1} s^{-1}, which was found when the entire kinetic system was fit to the multistep

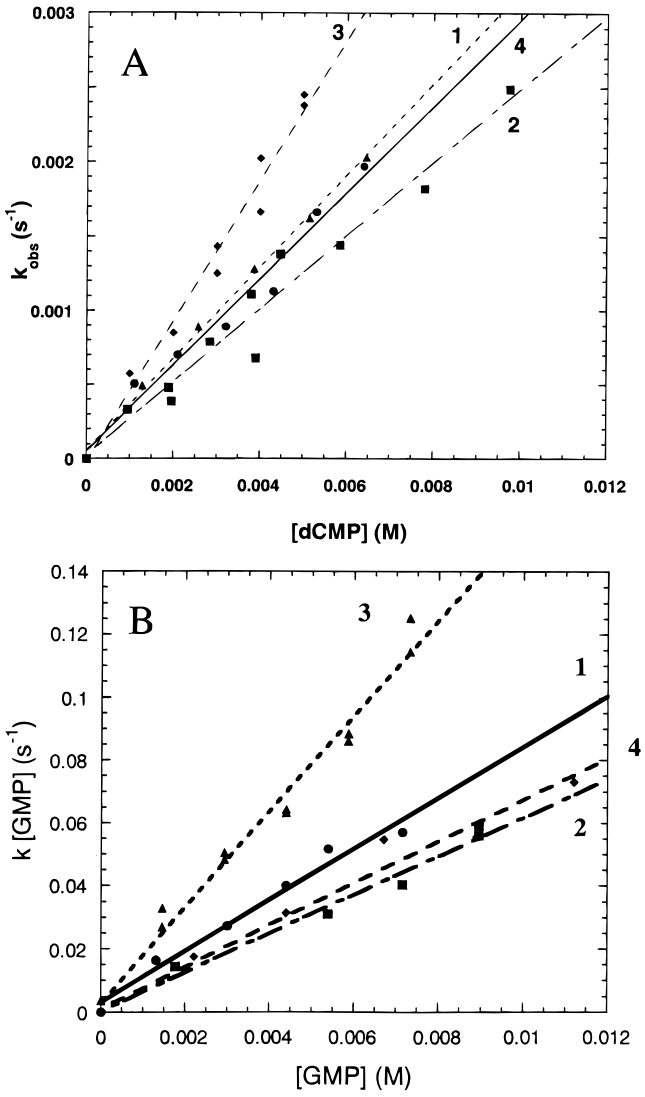

Figure 3. (A) Pseudo-first-order rate constants for oxidation of dCMP by compounds **1**−**4** in 50 mM sodium phosphate buffer (pH 7). (B) Initial rates for oxidation of GMP by compounds **1**−**4**. Lines are best linear fits to the experimental data that were used to determine the second-order rate constants in both (A) and (B).

mechanism.[20] Thus, initial rate analysis yields a rate constant for guanine oxidation that is identical within experiment error to that found from fitting the entire kinetic trace.

Plots of the initial rate vs [GMP] for all the complexes are shown in Figure 3B, and the results are given in Table 1. The guanine oxidation rate constants show the same trend as the sugar oxidation rate constants with **3** > **1** > **4** > **2**, indicating that a more electron-deficient oxo group increases the rate of reaction. Also shown in Table 1 are the ratios of the guanine and sugar rate constants (k_{gua}/k_{sug}).

Initial rate analysis was also performed for oxidation by Ru-(tpy)(bpy)O^{2+} of xanthosine 2′-monophosphate (XMP) and inosine 5′-monophosphate (IMP). The structures of xanthosine and hypoxanthine are similar to that of guanosine except in the 2 position of the purine ring where xanthine contains a carbonyl group and hypoxanthine contains only a hydrogen (Scheme 1; note that the base moiety of inosine is called hypoxanthine). IMP exhibits a higher ionization potential due to the absence of the electron-donating amino group than guanine,[24] and we

(22) Farrer, B. T.; Thorp, H. H. *Inorg. Chem.* **1999**, *38*, 2497−2502.
(23) Doddridge, Z. A.; Cullis, P. M.; Jones, G. D. D.; Malone, M. E. *J. Am. Chem. Soc.* **1998**, *120*, 10998−10999.
(24) Hush, N. S.; Cheung, A. S. *Chem. Phys. Lett.* **1975**, *34*, 11−13.

Scheme 1

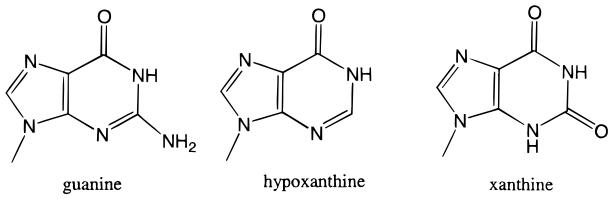

have shown that inosine is a much poorer one-electron donor than guanosine.[25] In contrast, xanthine exhibits a lower known ionization potential than guanine.[24,26] Reaction of XMP with $Ru(tpy)(bpy)O^{2+}$ proceeded with a much higher initial rate than GMP ($k = 85 \pm 5\ M^{-1}\ s^{-1}$), and IMP had a significantly slower rate. In fact, the reaction of IMP fit to the sugar oxidation mechanism (eqs 11 and 12) with a rate very similar to that of CMP. This finding suggests that oxidation of the hypoxanthine base is not competitive with oxidation of the 1′ C−H bond.

Oligonucleotide Oxidation. The oxidation of oligonucleotides and polynucleotides by oxoruthenium(IV) complexes produces direct strand cleavage resulting from the oxidation of the 1′ C−H bond and base-labile lesions resulting from guanine oxidation. In random coil DNA, the ratio of cleavage resulting from base and sugar oxidation corresponds to the ratio of the oxidation rates measured by stopped-flow spectrophotometry in experiments similar to those discussed above.[12] For double-stranded B-form DNA, formation of the three-dimensional structure occludes the 1′ C−H bond and the guanine base to different extents, which increases the ratio of sugar oxidation to guanine cleavage.[27] This effect is evident in comparing sequencing gels for the same oligonucleotide as a single strand or hybridized to its complement. This idea has been exploited in using these compounds to recognize highly reactive structures such as guanines in single-stranded loops and bulges within individual DNA or RNA molecules.[14,27]

The reaction of the $Ru(tpy)(bpy)O^{2+}$ derivatives with the 14-mer oligonucleotide 5′-ATGCCCTTGCGTAT (**DNA1**) was studied by high-resolution electrophoresis. Hybridization of **DNA1** to its complement, 5′-ATACGCAAGGGCAT (**DNA2**), was confirmed by following the absorption hypochromicity upon denaturation and rehybridization, which gave a T_m of 35 ± 3 °C. Competitive hybridization experiments were done with 5′-ATACGCAAGGGCATTACGGGACGCATA (**DNA3**) as a competitive complementary strand where **DNA1** was hybridized to either **DNA2** or **DNA3** by heating to 90 °C and slowly cooling (1 h) to 10 °C. The other strand was then added to the solution, and the products were separated on a 20% nondenaturing gel. The results demonstrate that less than 5% of **DNA1** is single-stranded under the conditions used for the RuO^{2+} cleavage reactions and that transfer of the DNA from one complement to another occurs more slowly than the time scale of the RuO^{2+} cleavage experiment, which is 10 min (gel given in the Supporting Information).

The extent of cleavage was determined by varying the amount of ruthenium oxidant and determining the change in cleavage with respect to ruthenium concentration. The resulting plots of cleavage intensity vs $[RuO^{2+}]$ were linear as long as the ruthenium concentration was kept sufficiently low. Throughout all experiments, the concentration of **DNA1** remained constant,

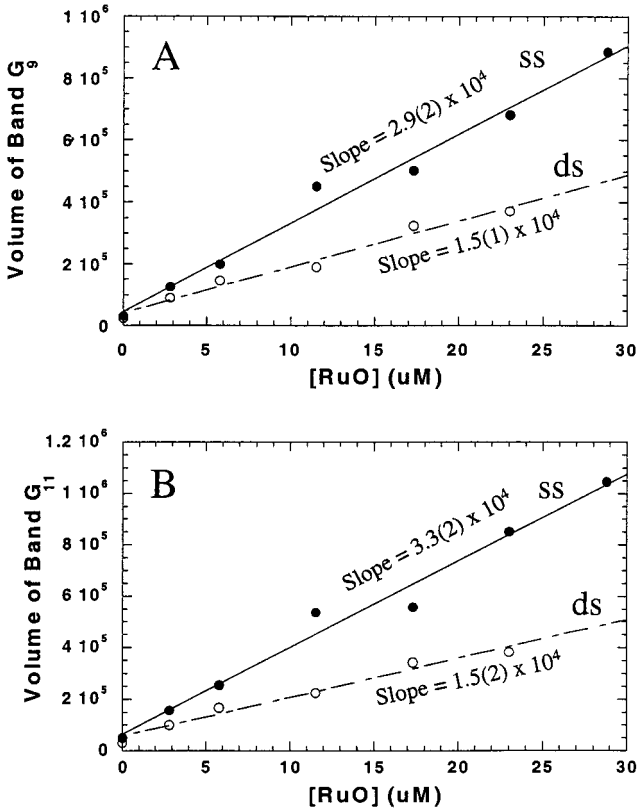

Figure 4. Integrated intensities at (A) G_9 and (B) G_{11} for oxidation by $Ru(tpy)(Me_2\text{-}bpy)O^{2+}$ as a function of ruthenium concentration.

so the total concentration of the DNA in the double-stranded reactions was a factor of 2.1 greater than in the single-stranded reactions (1.1 equiv of the unlabeled **DNA2** complement was used). The extent of oxidation at each nucleotide in **DNA1** by the ruthenium oxo compounds was determined by gel electrophoresis (gels are given in the Supporting Information). As an example, the absolute intensities of cleavage at G_{11} and G_9 for $Ru(tpy)(4,4'\text{-}Me_2\text{-}bpy)O^{2+}$ are shown in Figure 4 as a function of the metal concentration for **DNA1** and the **DNA1·DNA2** duplex. As shown, the slopes are decreased by approximately a factor of 2 in the hybridized case, which we assign to a simple doubling of the DNA concentration because there are two strands present.

Slopes for the extent of cleavage as a function of metal concentration were determined for the nucleotides G_{11}−T_7 for each metal complex as shown in Figure 4. The slopes for each nucleotide were normalized to that for G_{11}, which was generally the most reactive, and the results are given in the Supporting Information (Table S1). There is relatively little systematic change across the series of complexes with regard to selectivity for a given site. Comparison of the extent of guanine oxidation (G_{11} and G_9) with that of the sugar oxdiation (C_{10}, T_8, T_7) shows an increase in the relative contribution of sugar oxidation in the duplex form, as we have observed in other sequences and secondary structures.[27]

Discussion

We have discussed the mechanistic aspects of the reaction of the $Ru(IV)O^{2+}$ complexes with the guanine base elsewhere.[12] Small amounts of 8-oxoguanine have been detected in these reactions, although overoxidation by additional equivalents of both $Ru(IV)O^{2+}$ and $Ru(III)OH^{2+}$ prohibits assignment of 8-oxoguanine as the sole product.[12] The low potential of the

(25) Napier, M. E.; Loomis, C. R.; Sistare, M. F.; Kim, J.; Eckhardt, A. E.; Thorp, H. H. *Bioconjugate Chem.* **1997**, *8*, 906−913.
(26) Steenken, S.; Jovanovic, S. V. *J. Am. Chem. Soc.* **1997**, *119*, 617−618.
(27) Carter, P. J.; Cheng, C.-C.; Thorp, H. H. *Inorg. Chem.* **1996**, *35*, 3348−3354.

Table 2. Second-Order Rate Constants for Oxidation of Nucleotide Monophosphates by Ru(tpy)(bpy)O^{2+}

nucleotide	rate constant (M^{-1} s^{-1})	mechanism
guanosine 5′-monophosphate	8 ± 2^a	base oxidation
xanthosine 5′-monophosphate	85 ± 5^a	base oxidation
inosine 5′-monophosphate	0.11 ± 0.01^b	sugar oxidation
adenosine 5′-monophosphate	0.39 ± 0.03^b	sugar oxidation
deoxycytosine 5′-monophosphate	0.10 ± 0.01^b	sugar oxidation

[a] Determined by initial rate analysis; see the text. [b] Determined by fitting to the sugar oxidation mechanism given in eqs 11 and 12. Note that the experiments in this table are for ribonucleotides while the results for sugar oxidation in Table 1 are for 2′-deoxyribonucleotides.

IV/III and III/II couples for outer-sphere electron transfer (Table 1) precludes contribution from simple electron-transfer pathways,[28] as we have observed for $Ru(bpy)_3^{3+}$ [29,30] and many other groups have observed for other, equally potent outer-sphere oxidants.[4,31−34] Thus, guanine oxidation by Ru(tpy)(bpy)O^{2+} and related complexes must involve an inner-sphere pathway and not just simple outer-sphere electron transfer. Nonetheless, the trend in ionization potentials observed for the three guanine derivatives examined here (Scheme 1) follows the order xanthine < guanine < hypoxanthine,[24] which is the same order observed for oxidation by Ru(tpy)(bpy)O^{2+} in Table 2. So the reaction must involve a concerted action of the electrophilic oxo ligand and the oxidizing metal center. This idea is supported by the observation that the oxidation rate constants increase with the redox potentials, as shown in Table 1. The correlation of reaction rate with driving force for inner-sphere oxidation of organic substrates by oxo complexes is well-known.[35,36]

The sugar oxidation reaction proceeds with attack of the 1′ C−H bond to form methylenefuranone (eq 1). We have shown previously that this reaction proceeds with transfer of labeled oxo ligand from Ru(tpy)(bpy)O^{2+} into the organic product.[13] Further, we have demonstrated that polar substituents on the 2′ position of the nucleic acid reduce the reactivity in a manner consistent with a polar Hammett correlation ($\rho = -1.7$).[37] Here we show that substituents on the polypyridyl rings of the oxidant exert a relatively modest effect on the rate constant, far lower than the influence of substituents at the 2′-position in the nucleic acid. Again, this finding supports a reaction mechanism where inner-sphere addition of the oxo ligand is coupled to the effect of the multielectron metal oxidant.

A number of oxidants, especially oxometal species, oxidize DNA via multiple pathways, often including parallel base and sugar oxidation or oxidation of the sugar at multiple sites. For example, the oxomanganese porphyrins oxidize DNA at both the 1′ and 5′ sites,[6,38] and oxochromium complexes exhibit base and sugar reaction pathways.[10] Likewise, complexes based on Ru(tpy)(bpy)O^{2+} exhibit parallel guanine and 1′ sugar oxidation pathways that compete on the basis of their innate relative rates, the binding preferences of the complex, and the solvent accessibility of the oxidized site. We have demonstrated elsewhere that when a relatively large number of nucleotides in a single-stranded oligomer are followed, that the ratio of cleavage at guanine and sugar is similar to the ratio of rate constants for guanine and sugar oxidation in mononucleotides (i.e., Table 1).[27] Here, we show that, at low ruthenium concentrations, the extent of cleavage depends linearly on the ruthenium concentration, as would be expected if the chemical oxidation step is rate-limiting. We have shown previously that this behavior persists when substitutions are made on the 2′ position of the sugar,[37] and here we show that similar linear behavior is observed when substitutions are made at the metal complex.

A final noteworthy point centers on the parallels between the changes in the guanine and sugar pathways observed in mononucleotides and on the sequencing gels. We have shown previously that changes in the available oxidizing pathways of the metal−oxygen functionality that produce detectable changes in the guanine and sugar oxidation rates are readily detected in the sequencing gels.[12] For example, reaction of Ru(III)OH^{2+} analogues produces only guanine oxidation, and in parallel, the Ru(III)OH^{2+} species are only competent to oxidize guanine in mononucleotides and not sugar.[12] Likewise, attenuation of the sugar pathway by addition of a polar substituent at the 2′-position of the sugar shuts off the sugar oxidation both on sequencing gels and in kinetics studies.[13,37] Here we show that oxidation of hypoxanthine is not competitive with sugar oxidation in kinetics studies (Table 2), and we have shown elsewhere that substitution of hypoxanthine for guanine eliminates base oxidation by Ru(tpy)(bpy)O^{2+} on sequencing gels.[37] Finally, we show that the substitutions on the metal complex lead to modest changes in the overall reactivity and in the guanine/sugar ratio in kinetic studies (Table 1) and similarly to modest changes in the guanine/sugar ratio observed on sequencing gels. Thus, the observation of extents of cleavage on sequencing gels is a reliable measure of the true reactivity of the Ru(tpy)(bpy)O^{2+} complexes in solution determined using real-time methods.

Acknowledgment. We thank the National Science Foundation for support of this research. B.T.F. thanks the Department of Education for a GAANN Fellowship.

Supporting Information Available: Table of relative extents of cleavage at individual nucleotides for the five complexes in the double-stranded oligomer, optical spectra of the Ru(II), Ru(III), and Ru(IV) forms, native gel showing the extent of hybridization of **DNA1** and **DNA2**, and high-resolution polyacrylamide gels showing the cleavage of **DNA1** by the substituted complexes. This material is available free of charge via the Internet at http://pubs.acs.org.

IC990833U

(28) Meyer, T. J. *J. Electrochem. Soc.* **1984**, *131*, 221C.
(29) Johnston, D. H.; Glasgow, K. C.; Thorp, H. H. *J. Am. Chem. Soc.* **1995**, *117*, 8933−8938.
(30) Ropp, P. A.; Thorp, H. H. *Chem. Biol.* **1999**, *6*, 599−605.
(31) Lewis, F. D.; Wu, T.; Zhang, Y.; Letsinger, R. L.; Greenfield, S. R.; Wasielewski, M. R. *Science* **1997**, *277*, 673−676.
(32) Gasper, S. M.; Schuster, G. B. *J. Am. Chem. Soc.* **1997**, *119*, 12762−12771.
(33) Hall, D. B.; Holmlin, R. E.; Barton, J. K. *Nature* **1996**, *384*, 731−735.
(34) Saito, I.; Takayama, M.; Sugiyama, H.; Nakatani, K.; Tsuchida, A.; Yamamoto, M. *J. Am. Chem. Soc.* **1995**, *117*, 6406−6405.
(35) Garrison, J. M.; Ostovic, D.; Bruice, T. C. *J. Am. Chem. Soc.* **1989**, *111*, 4960−4966.
(36) Acquaye, J. H.; Muller, J. G.; Tackeuchi, K. J. *Inorg. Chem.* **1993**, *32*, 160−165.
(37) Farrer, B. T.; Pickett, J. S.; Thorp, H. H. *J. Am. Chem. Soc.*, in press.
(38) Pratviel, G.; Pitié, M.; Bernadou, J.; Meunier, B. *Angew. Chem., Int. Ed. Engl.* **1991**, *30*, 702−703.